

# Transmission Geometry Laserspray Ionization *Vacuum* Using an Atmospheric Pressure Inlet

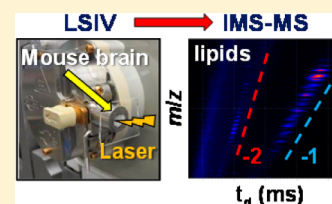
Corinne A. Lutomski,<sup>†,§</sup> Tarick J. El-Baba,<sup>†,§</sup> Ellen D. Inutan,<sup>†</sup> Cory D. Manly,<sup>†</sup> James Wager-Miller,<sup>‡</sup> Ken Mackie,<sup>‡</sup> and Sarah Trimpin<sup>\*,†</sup>

<sup>†</sup>Department of Chemistry, Wayne State University, Detroit, Michigan 48202, United States

<sup>‡</sup>Gill Center for Biomolecular Science, Indiana University, Bloomington, Indiana 47405, United States

## Supporting Information

**ABSTRACT:** This represents the first report of laserspray ionization *vacuum* (LSIV) with operation directly from atmospheric pressure for use in mass spectrometry. Two different types of electrospray ionization source inlets were converted to LSIV sources by equipping the entrance of the atmospheric pressure inlet aperture with a customized cone that is sealed with a removable glass plate holding the matrix/analyte sample. A laser aligned in transmission geometry (at 180° relative to the inlet) ablates the matrix/analyte sample deposited on the vacuum side of the glass slide. Laser ablation from vacuum requires lower inlet temperature relative to laser ablation at atmospheric pressure. However, higher inlet temperature is required for high-mass analytes, for example,  $\alpha$ -chymotrypsinogen (25.6 kDa). Labile compounds such as gangliosides and cardiolipins are detected in the negative ion mode directly from mouse brain tissue as intact doubly deprotonated ions. Multiple charging enhances the ion mobility spectrometry separation of ions derived from complex tissue samples.



In laserspray ionization (LSI), matrix/analyte sample is ablated into the vacuum of a mass spectrometer producing ions with charge states similar to electrospray ionization (ESI). LSI is distinguished as LSII when the sample is ablated at atmospheric pressure into a heated *inlet* tube of a mass spectrometer,<sup>1</sup> and laserspray ionization *vacuum* (LSIV) is when the sample is ablated in *vacuum*.<sup>2</sup> The analyte ion abundance observed is a function of the inlet temperature as well as voltages normally applied to increase ion fragmentation and surface collisions.<sup>3–5</sup> The combination of heat, applied voltage, and collisions are thought to assist in removing the matrix from the charged matrix/analyte clusters, similar to desolvation in ESI.<sup>1–8</sup>

LSIV has been demonstrated on commercial vacuum matrix-assisted laser desorption/ionization (MALDI) sources operating with the laser aligned in reflection geometry.<sup>2,9,10</sup> At intermediate pressure (0.16 Torr), LSIV produces results nearly identical to LSII, but without a heated inlet tube and lower laser fluences than used in MALDI.<sup>2,3,10</sup> However, operation from vacuum using an ion source built for MALDI analyses has the disadvantages of requiring several minutes to insert and remove samples, and only a limited number of matrices are capable of producing multiply charged ions at intermediate pressure.<sup>5,9</sup> These matrices include 2,5-dihydroxyacetophenone (2,5-DHAP)<sup>2,11</sup> and 2-nitrophenolglucosyl (2-NPG).<sup>9,11</sup> In LSIV, it is assumed that matrix must be evaporated or sublimed from charged clusters to produce the multiply charged ions, and this is facilitated by the use of more volatile matrices. Energy for “desolvation” is available through absorption of the laser, rf voltages, gas or physical collisions, and the low pressure conditions,<sup>2,5,9</sup> but it is often insufficient to remove matrix from

the less volatile charged clusters.<sup>3,12</sup> Both 2,5-DHAP and 2-NPG require the inlet tube to be heated for efficient ionization when ablated at atmospheric pressure using LSII.<sup>9,11</sup>

Because the initial work with LSII used a hot inlet tube to produce ions, the method was limited to instruments having inlet tubes that can be significantly heated.<sup>1,5</sup> Mass spectrometers with skimmer inlets, such as the Waters Z-Spray ion source, required construction of a heated inlet tube<sup>13</sup> which has been adapted to other sources.<sup>4</sup> However, using more volatile matrices, the applicability of LSIV can be extended without requiring extensive heat. 3-Nitrobenzotrile (3-NBN), which sublimates at room temperature, was found to produce ions when incorporated with the analyte without the use of a laser, voltage, or additional heat when exposed to subatmospheric pressure.<sup>14</sup> The energy contained in the matrix is sufficient for analyte ionization and has been discussed to be related to luminescence characteristics of the small molecule compound.<sup>12,14</sup> This matrix has been shown to produce multiply charged analyte ions when introduced to a vacuum using an intermediate pressure MALDI source<sup>14</sup> or directly from atmospheric pressure into an inlet aperture.<sup>15</sup> Even though a laser is not necessary for ionization using 3-NBN as matrix, there are applications where use of a laser is desirable, such as sampling small areas and in imaging studies.<sup>10,16–24</sup> Additionally, aligning the laser in transmission geometry (180° relative to the inlet) is desirable for applications that require higher spatial resolution<sup>20</sup> and speed of analysis.<sup>25</sup>

Received: February 11, 2014

Accepted: June 4, 2014

Published: June 4, 2014

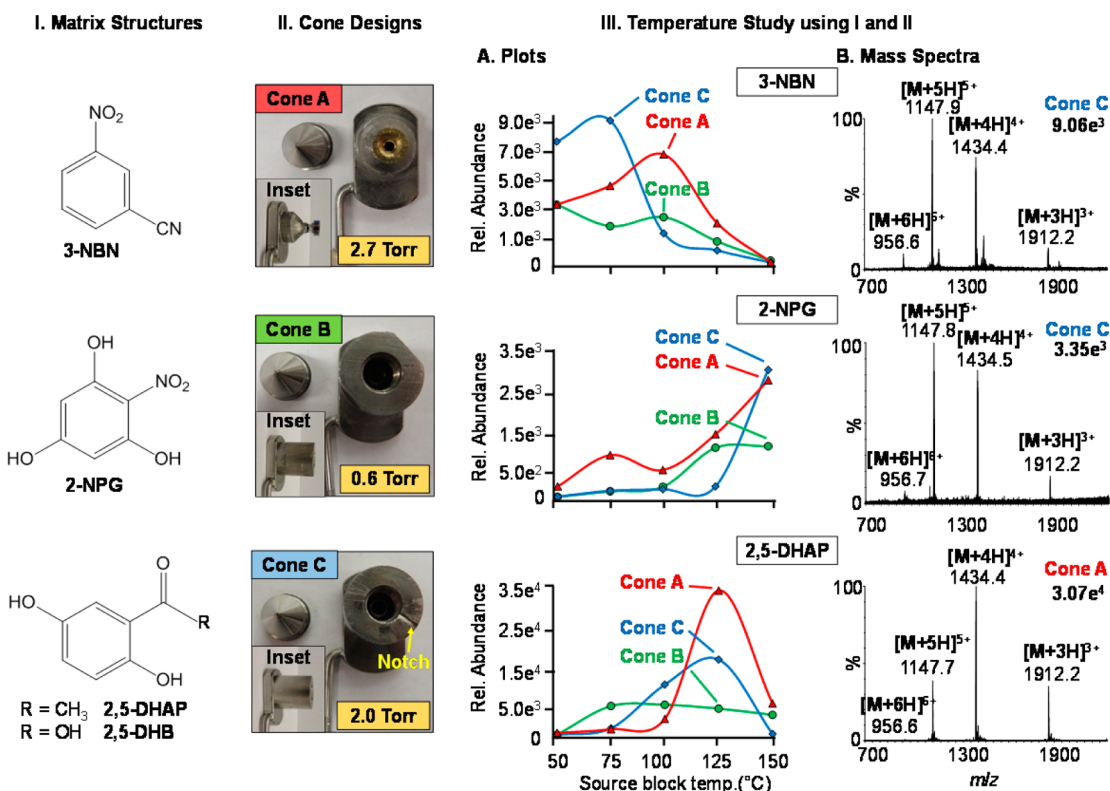


**Figure 1.** Source performance relative to different matrices, cones, and temperatures. (I) Matrix structures: 3-nitrobenzonitrile (3-NBN), 2-nitrophenol (2-NPG), 2,5-dihydroxyacetophenone (2,5-DHAP), and 2,5-dihydroxybenzoic acid (2,5-DHB). (II) Different cone designs including Cone A at ~2.7 Torr, Cone B at ~0.6 Torr, and Cone C at ~2.0 Torr. Inset photographs show side view of cones and pressure values obtained from the backing pressure vacuum gauge of the SYNAPT G2. (III) Temperature study using matrix compounds from (I) and (II) cone designs A–C. (III.A) Plots of temperature vs relative ion abundance of the  $[M + 5H]^{5+}$  charge state of bovine insulin on the different cone designs: Cone A (triangle), Cone B (circle), and Cone C (diamond) and (III.B) representative mass spectra. Additional mass spectral data provided in Figures S5–S7, Supporting Information.

Here, we report studies in which the atmospheric pressure inlets of two mass spectrometers were modified to allow matrix/analyte sample to be ablated at reduced pressure. Using laser ablation in transmission geometry, the applicable mass range relative to previously reported LSIV measurements was extended. Further, the inlet temperature could be reduced relative to LSII, thereby extending the method to instruments without a heated inlet tube. The new inlet design achieves analyses directly from laser ablation of mouse brain tissue sections, and changing samples becomes fast and simple with this approach.

## EXPERIMENTAL SECTION

**Materials.** Matrix compounds 3-NBN, 2-NPG, and 2,5-DHB were purchased from Sigma-Aldrich (St. Louis, MO). 2,5-DHAP was purchased from Acros Organics (Fairlawn, NJ). More details about sample preparation of the mouse brain tissue section and purchased standards including lipids, peptides, and proteins can be found in the Supporting Information. All procedures involving mice were approved by the Indiana University Bloomington Institutional Animal Care and Use Committee.

**Mass Spectrometers, Ion Sources, and Methods.** LSIV and LSII were performed on the Z-Spray ion source of the SYNAPT G2 (Waters Corporation, Milford, MA) and the Ion Max source of the LTQ Velos (Thermo, Bremen, Germany) mass spectrometers. For open access to the mass spectrometer inlet apertures, the exterior housing of the ESI sources were

detached and interlocks were overridden as previously described.<sup>13,20</sup> The laser (337 nm N<sub>2</sub> laser, Newport Corporation, Irvine, CA) was aligned in transmission geometry and used to dislodge the matrix/analyte from the surface of the glass plate into the vacuum using a repetition rate of 3 to 4 Hz. A glass slide (Gold Seal, Portsmouth, NJ), transmitting at the laser wavelength, was used as the sample holder and a lens enabled focusing of the laser beam, as previously employed for LSII.<sup>20,26</sup> The ablation of different areas of the stationary glass plate was achieved either by slightly moving the lens parallel to the laser beam or by rotating the sample plate. The source block temperature of the SYNAPT G2 was varied from 50 to 150 °C, and the inlet tube temperature on the LTQ Velos was varied from 50 to 450 °C.

A series of inlet cones was designed to be used on the Z-Spray ion source of the SYNAPT G2 in place of the skimmer inlet. The glass slide holding the matrix/analyte sample adhered to the surface of each respective cone by the pressure differential between atmospheric pressure and the vacuum at the inlet. The first cone (Cone A) was modified by widening the orifice and equipping the aperture with a connecting home-built stainless steel extension 7 mm long with a 4 mm diameter opening. The loosely connected extension has a flat outer surface capable of creating a vacuum seal (~2.7 Torr), but it did not entirely restrict the air flow to the inlet. Another cone design (Cone B) consisted of an airtight (~0.6 Torr) stainless steel cylinder extending 15 mm with an opening diameter of 7 mm. A third cone (Cone C), similar to Cone B, had a notch

approximately 1 mm wide and 0.5 mm deep cut into the outer surface of the cone to provide an air flow between the glass sample holder and the inner cone ( $\sim 2.0$  Torr). The reported pressure values are an average of pressures obtained from the backing pressure display on the Waters SYNAPT G2. There was little variation in pressure observed for each respective cone with the changes in source block temperature.

## RESULTS AND DISCUSSION

The sample holder and modified atmospheric pressure Ion Max heated inlet tube (Thermo) and Z-Spray (Waters) sources are

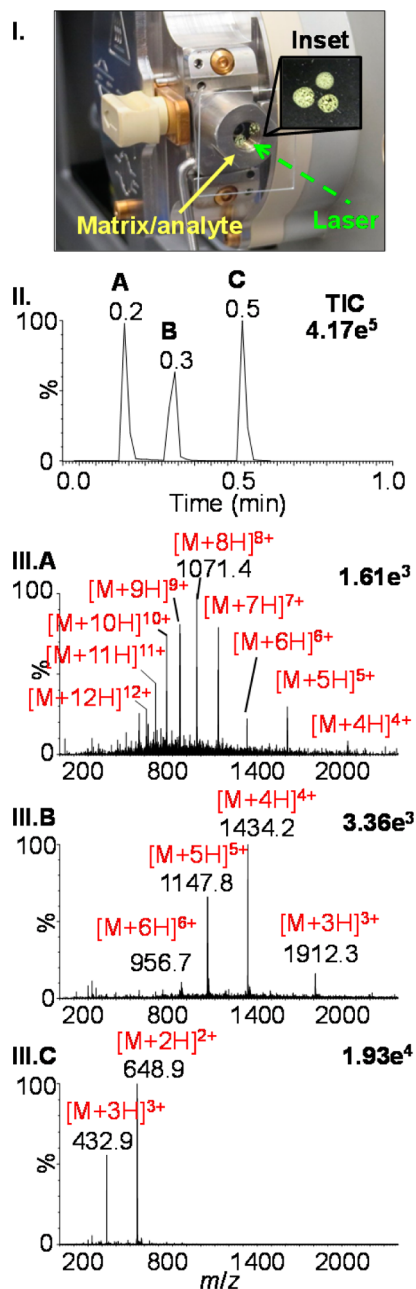


**Figure 2.** Transmission geometry LSIV of three consecutive analytes using matrix 2,5-DHAP (I) photo and inset of sample placement, (II) total ion chromatogram (TIC), and (III) mass spectra: (A) ubiquitin (MW, 8565), (B) bovine insulin (MW, 5730), and (C) angiotensin I (MW, 1295). Data obtained on a Z-Spray ion source of a Waters SYNAPT G2 and a source temperature of 125 °C using Cone C.

shown in Schemes S1 and S2, Supporting Information, respectively. On both sources, the laser ablation of the matrix/analyte sample occurred under subsambient pressure. Direct comparison between this LSIV approach and LSII was achieved by adhering the glass plate to the inlet attachment by the vacuum differential (Scheme S1A, Supporting Information) or by placing the plate in near proximity to the heated inlet aperture of an LTQ Velos (Scheme S1B, Supporting Information) as previously reported for LSII<sup>1</sup> so that matrix ablation occurs at atmospheric pressure. The matrix compounds 3-NBN, 2-NPG, 2,5-DHAP, and 2,5-DHB (Figure 1I) were selected on the basis of previous applicability.<sup>1,9,11,14</sup> The observed ion abundance on average is lower with LSIV as compared to LSII, but the chemical background is also lower. The results (Figures S1–S4, Supporting Information) demonstrate that lower temperature can be employed using vacuum assistance, which is important for ion sources having limited heating capabilities.

The LSIV source constructed onto a Z-Spray inlet aperture of a Waters SYNAPT G2 (graphical abstract) can be heated to 150 °C. Different cones (Figure 1II) exposed the matrix/analyte to different pressures. Cones A and C provided air flow through the loosely fitted cone attachment or a notched surface, respectively. The airtight Cone B maintained the lowest pressure of  $\sim 0.6$  Torr and provided the least air flow to the matrix/analyte sample and through the Z-Spray source.

The same four matrix compounds (Figure 1I) were used to study the effect of varying the source block temperature from 150 to 50 °C using bovine insulin as analyte. The results (Figure 1III) varied for the different matrices using the three different cones (Figure 1II). The least volatile of the matrices studied, 2,5-DHB, did not produce ions from bovine insulin on any of the cone designs up to the maximum source temperature of 150 °C. The most volatile of the matrices, 3-NBN (Figure 1III.A), produced the highest ion abundance of the  $[M + 5H]^{5+}$  charge state at a source temperature of 75 °C using the notched Cone C and failed to produce meaningful analyte ions on all cone designs at the maximum source temperature of 150 °C; the intolerance of this matrix to heat has been previously described.<sup>14,15</sup> It should be noted that, with Cone C, 3-NBN did not spontaneously sublime as in the matrix assisted ionization *vacuum* (MAIV) method.<sup>14,15</sup>

The 2-NPG matrix required the highest available source temperature of 150 °C, while 2,5-DHAP provided the highest analyte ion intensity at a source temperature of 125 °C. The airtight Cone B (Figure 1III.A, green plot lines) provided the lowest analyte ion abundance for all matrices when compared to Cones A (Figure 1III.A, red plot lines) and C (Figure 1III.A, blue plot lines) suggesting the importance of air flow in ion transmission and possibly aiding the ionization process.<sup>3,12</sup> This might be expected since the Z-Spray source is designed to operate with rather high gas flow. The representative mass spectra (Figure 1III.B) are shown corresponding to the highest ion intensity of the  $[M + 5H]^{5+}$  charge state observed for bovine insulin using each matrix. There is little to no chemical background observed in the mass spectrum, contrary to MALDI experiments.

The ion abundance and shape of the plotted total ion chromatogram (TIC) varied across the different temperatures, pressures, and matrices used (Figures S8–S10, Supporting Information). The most volatile of the matrices, 3-NBN, produced sharp peaks after each laser ablation using all three cones at temperatures between 50 and 100 °C, as shown in the

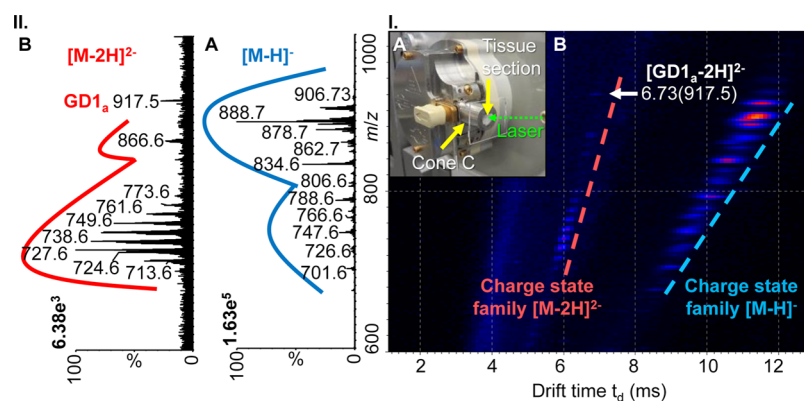


**Figure 3.** Transmission geometry LSIV-IMS-MS directly from mouse brain tissue in negative ion mode. (I.A) Photo of entrance region of the LSIV source with a mouse brain tissue section on a glass plate adhered to Cone C. (I.B) 2-D plot of drift time versus  $m/z$  with lines indicating separated charge state families. (II) Extracted mass spectra: (II.A)  $[M - H]^{-}$  and (II.B)  $[M - 2H]^{2-}$  charge state families. Data was obtained using the Z-Spray ion source of the Waters SYNAPT G2 with matrix 3-NBN at a source temperature of 80 °C. Details of tentative lipid assignments are provided in Figure S12, Supporting Information. Mass spectra and drift times of GD1 standards are provided in Figures S13 and S14, Supporting Information.

TIC (Figure S8A–C, Supporting Information). However, at temperatures above 125 °C, the matrix began to visually sublime from the plate and only a low abundant continuum of ion formation was observed (Figure S8D,E, Supporting Information). Conversely, 2,5-DHAP required higher temperatures with a minimum of 100 °C for abundant analyte ion observation (Figure S9E, Supporting Information). Although the matrix 2-NPG did not produce sharp peaks in the TIC (Figure S10, Supporting Information), it produced high analyte ion abundance at a source temperature of 150 °C using all three cone designs (Figure S6E, Supporting Information).

Studies conducted in the negative mode also showed that 3-NBN required a low source temperature for ionization. For example, multiply charged deprotonated ions for bovine insulin up to  $[M - 6H]^{6-}$  charge states are observed at a temperature of 50 °C (Figure S11A, Supporting Information). Previous studies using MAIV demonstrated that this matrix efficiently ionizes ubiquitin with  $-8$  charges (8.5 kDa) in the negative mode and higher mass proteins (66 kDa) up to  $[M + 36H]^{36+}$  in the positive mode using conditions that permit spontaneous ionization without the use of a laser.<sup>14</sup> The stability of this matrix under the LSIV conditions using Cone C comes at the expense of more limited mass range relative to the spontaneous ionization of MAIV.

2,5-DHAP which is less volatile than 3-NBN allows flexibility in temperature, air-flow, and pressure. With 2,5-DHAP, LSIV can be extended to higher mass proteins such as  $\alpha$ -chymotrypsinogen. Multiply charged ions up to  $[M + 19H]^{19+}$  were produced for this 25.6 kDa protein using Cone C at a source temperature of 125 °C (Figure S11B, Supporting Information). On the atmospheric pressure source of the same mass spectrometer, previous LSIV investigations using 2,5-DHAP required a retrofitted inlet tube heated by the source block at a temperature of 150 °C to produce multiply charged ions of lysozyme (14.3 kDa) with 14 charges.<sup>27</sup> Using the same matrix on the commercial intermediate pressure ( $\sim 0.16$  Torr) source of the same mass spectrometer, the highest mass protein observed was ubiquitin (8.5 kDa), producing multiply charged ions up to  $[M + 12H]^{12+}$ .<sup>2</sup> This relates well with the hypothesis that “desolvation” of the charged matrix/analyte clusters is necessary to expose bare analyte ions.<sup>3,12</sup>

To investigate the prospect of fast analyses, ubiquitin, bovine insulin, and angiotensin I were individually spotted onto a glass

microscopy slide in a triangular shape and layered with a solution of 2,5-DHAP and dried (Figure 2I). Manual rotation of the sample plate on the cone allowed three separate laser shots to ablate an area of each individual matrix/analyte spot. The TIC shows three distinct peaks corresponding to the sequential ionization of the samples in about 18 s (Figure 2II). Summing acquisitions for each individual peak, the mass spectra of ubiquitin (Figure 2III.A), bovine insulin (Figure 2III.B), and angiotensin I (Figure 2III.C) were obtained with good analyte ion intensity. Importantly, no carry-over is observed between samples when loading 1 pmol of analyte.

The utility of transmission geometry LSIV is demonstrated using a 10  $\mu$ m thick mouse brain tissue section. 3-NBN matrix solution was spotted directly onto the tissue surface, and the glass slide was placed on the flat outer surface of Cone C. The cone opening encloses the mouse brain tissue section (Figure 3I.A) while still providing stability of the volatile 3-NBN matrix to not spontaneously sublime from the surface. The laser beam was rastered across the surface of the mouse brain tissue coated with matrix by manually moving the focusing lens perpendicular to the laser beam. Abundant singly and doubly deprotonated negatively charged ions of lipids (Figure S12A, Supporting Information) were observed at a source temperature of 80 °C.

The multiply charged ions show enhanced IMS separation relative to singly charged ions allowing for straightforward observation and clean extraction of charge state families from the 2-dimensional plot of drift time vs mass-to-charge ratio ( $m/z$ ) (Figure 3I.B). The extracted singly charged lipids (Figure 3II.A) were tentatively assigned as sulfatides, phosphatidylserines, phosphatidylethanolamines, phosphatidic acids, and sphingomyelins with varying lipid chain lengths (Figure S12B.I, Supporting Information).<sup>28–31</sup> The doubly deprotonated lipids (Figure 3II.B) were tentatively assigned as cardiolipins and disialogangliosides (GD1) (Figure S12B.2, Supporting Information).<sup>22,32,33</sup> It is important to note that the analysis of intact gangliosides by intermediate pressure LSIV and MALDI previously failed on the same mass spectrometer.<sup>22</sup>

In addition to the separation provided by IMS, unique mobility values can be extracted from the 2-dimensional plot and displayed as a “nested data set” of  $t_d(m/z)$ ,<sup>34,35</sup> which is especially important when considering species that exist as isomers such as gangliosides.<sup>22</sup> Each ganglioside isomer has an

individual drift time leading to the observation of differences in mobility rather than  $m/z$  for GD1<sub>a</sub> (Figure S13IA, Supporting Information) and GD1<sub>b</sub> (Figure S13IB, Supporting Information) at 6.73(917.5) and 6.62(917.5), respectively. By comparing the drift times of the standards with the lipid detected at a drift time of 6.73 ms in the mouse brain tissue section (Figure S14, Supporting Information), the GD1<sub>a</sub> isomer is tentatively assigned to the doubly deprotonated ion in Figure 3II.B at  $m/z$  917.5.

## CONCLUSIONS

This work demonstrates that LSIV can be achieved on atmospheric pressure sources using a simple modification. Heat applied to the source is shown to be an important parameter, and it is suggested that this will also be the case applying heat to an intermediate pressure MALDI source. Therefore, with proper engineering, a heated LSIV source, with laser aligned in transmission<sup>1,13</sup> or reflection geometry,<sup>2,11</sup> can be constructed to take advantage of the high ion transmission of vacuum sources relative to atmospheric pressure sources.<sup>36</sup> This heated LSIV source can provide convenient and rapid sample introduction and be capable of using volatile matrix compounds such as 3-NBN to eliminate matrix related instrument contamination. In addition, the combination of heat and vacuum extends the applicable mass range of previous LSIV and LSII approaches,<sup>2,9,13,27</sup> as well as making the method softer<sup>22</sup> using the same mass spectrometer. The laser aligned in transmission geometry offers speed of analysis,<sup>25</sup> and the simple movement of the focusing lens held at atmospheric pressure will allow high repetition mass measurements of surfaces potentially suitable for surface imaging.<sup>10,20,22,24</sup>

## ASSOCIATED CONTENT

### Supporting Information

Additional information as noted in the text. This material is available free of charge via the Internet at <http://pubs.acs.org>.

## AUTHOR INFORMATION

### Corresponding Author

\*E-mail: [stimpin@chem.wayne.edu](mailto:stimpin@chem.wayne.edu).

### Author Contributions

§C.A.L. and T.J.E.-B. contributed equally. The manuscript was written through contributions of all authors. All authors have given approval to the final version of the manuscript.

### Notes

The authors declare no competing financial interest.

## ACKNOWLEDGMENTS

The authors are thankful for financial support from NSF CAREER 0955975, ASMS Research Award, DuPont Young Professor Award, Waters Center of Innovation Program, Eli Lilly Young Investigator Award in Analytical Chemistry (to S.T.), and NIH grants DA011322 and DA021696 (to K.M.), as well as WSU (Summer Undergraduate Fellowship to C.D.M., Summer Dissertation, Rumble, and Schaap Graduate Fellowships to E.D.I. and Schaap Faculty Scholar to S.T.). We acknowledge Jeff Brown (Waters) for providing the potential LSII connector, Christopher B. Lietz (WSU) for his perseverance in evaluating the connector assembly for LSII, and Dr. Charles McEwen (U. Sciences, Philadelphia, PA) for constructive feedback on this manuscript.

## REFERENCES

- (1) Trimpin, S.; Inutan, E. D.; Herath, T. N.; McEwen, C. N. *Mol. Cell. Proteomics* **2010**, *9*, 362–367.
- (2) Inutan, E. D.; Wang, B.; Trimpin, S. *Anal. Chem.* **2011**, *83*, 678–684.
- (3) Trimpin, S.; Wang, B.; Inutan, E. D.; Li, J.; Lietz, C. B.; Harron, A.; Pagnotti, V. S.; Sardelis, D.; McEwen, C. N. *J. Am. Soc. Mass Spectrom.* **2012**, *23*, 1644–1660.
- (4) Nyadong, L.; Inutan, E. D.; Wang, X.; Hendrickson, C. L.; Trimpin, S.; Marshall, A. G. *J. Am. Soc. Mass Spectrom.* **2013**, *24*, 320–328.
- (5) Li, J.; Inutan, E. D.; Wang, B.; Lietz, C. B.; Green, D. R.; Manly, C. D.; Richards, A. L.; Marshall, D. D.; Lingenfelter, S.; Ren, Y.; Trimpin, S. *J. Am. Soc. Mass Spectrom.* **2012**, *23*, 1625–1643.
- (6) Frankevich, V.; Nieckarz, R. J.; Sagulenko, P. N.; Barylyuk, K.; Zenobi, R.; Levitsky, L. I.; Agapov, A. Y.; Perlova, Y. T.; Gorshkov, M. V.; Tarasova, I. A. *Rapid Commun. Mass Spectrom.* **2012**, *26*, 1567–1572.
- (7) Musapelo, T.; Murray, K. K. *Rapid Commun. Mass Spectrom.* **2013**, *27*, 1283–1286.
- (8) Musapelo, T.; Murray, K. K. *J. Am. Soc. Mass Spectrom.* **2013**, *24*, 1108–1115.
- (9) Trimpin, S.; Ren, Y.; Wang, B.; Lietz, C. B.; Richards, A. L.; Marshall, D. D.; Inutan, E. D. *Anal. Chem.* **2011**, *83*, 5469–5475.
- (10) Inutan, E. D.; Wager-Miller, J.; Mackie, K.; Trimpin, S. *Anal. Chem.* **2012**, *84*, 9079–9084.
- (11) McEwen, C. N.; Larsen, B. S.; Trimpin, S. *Anal. Chem.* **2012**, *82*, 4998–5001.
- (12) Trimpin, S.; Wang, B.; Lietz, C. B.; Marshall, D. D.; Richards, A. L.; Inutan, E. D. *Crit. Rev. Biochem. Mol. Biol.* **2013**, *48*, 409–429.
- (13) Inutan, E. D.; Trimpin, S. *J. Am. Soc. Mass Spectrom.* **2010**, *21*, 1260–1264.
- (14) Inutan, E. D.; Trimpin, S. *Mol. Cell. Proteomics* **2013**, *12*, 792–796.
- (15) Trimpin, S.; Inutan, E. D. *Anal. Chem.* **2013**, *85*, 2005–2009.
- (16) Galicia, M. C.; Vertes, A.; Callahan, J. H. *Anal. Chem.* **2002**, *74*, 1891–1895.
- (17) McLean, J. A.; Russell, W. K.; Russell, D. H. *Anal. Chem.* **2003**, *75*, 648–654.
- (18) Kiss, A.; Heeren, R. M. A. *Anal. Bioanal. Chem.* **2011**, *399*, 2624–2634.
- (19) Inutan, E. D.; Richards, A. L.; Wager-Miller, J.; Mackie, K.; McEwen, C. N.; Trimpin, S. *Mol. Cell. Proteomics* **2011**, *10*, 1–8.
- (20) Richards, A. L.; Lietz, C. B.; Wager-Miller, J. B.; Mackie, K.; Trimpin, S. *Rapid Commun. Mass Spectrom.* **2011**, *25*, 815–820.
- (21) Schober, Y.; Guenther, S.; Spengler, B.; Roempp, A. *Anal. Chem.* **2012**, *84*, 6293–6297.
- (22) Richards, A. L.; Lietz, C. B.; Wager-Miller, J.; Mackie, K.; Trimpin, S. *J. Lipid Res.* **2012**, *53*, 1390–1398.
- (23) Zavalin, A.; Todd, E. M.; Rawhouser, P. D.; Yang, J.; Norris, J. L.; Caprioli, R. M. *J. Mass Spectrom.* **2012**, *47*, 1473–1481.
- (24) Harron, A. F.; Hoang, K.; McEwen, C. N. *Int. J. Mass Spectrom.* **2013**, *352*, 65–69.
- (25) Richards, A. L.; Marshall, D. D.; Inutan, E. D.; McEwen, C. N.; Trimpin, S. *Rapid Commun. Mass Spectrom.* **2011**, *25*, 247–250.
- (26) Trimpin, S.; Inutan, E. D.; Herath, T. N.; McEwen, C. N. *Anal. Chem.* **2010**, *82*, 11–15.
- (27) Inutan, E. D.; Trimpin, S. *J. Proteome Res.* **2010**, *9*, 6077–6081.
- (28) Paglia, G.; Ifa, D. R.; Wu, C. P.; Corso, G.; Cooks, R. G. *Anal. Chem.* **2010**, *82*, 1744–1750.
- (29) Angel, P. M.; Spraggins, J. M.; Baldwin, H. S.; Caprioli, R. *Anal. Chem.* **2012**, *84*, 1557–1564.
- (30) Thomas, A.; Charbonneau, J. L.; Fournaise, E.; Chaurand, P. *Anal. Chem.* **2012**, *84*, 2048–2054.
- (31) Cerruti, C. D.; Benabdellah, F.; Laprevote, O.; Touboul, D.; Brunelle, A. *Anal. Chem.* **2012**, *84*, 2164–2171.
- (32) Valianpour, F.; Wanders, R. J. A.; Barth, P. G.; Overmars, H.; Van Gennip, A. H. *Clin. Chem.* **2002**, *48*, 1390–1397.

- (33) Kiebish, M. A.; Han, X.; Cheng, H.; Chuang, J. H.; Seyfried, T. *N. J. Lipid Res.* **2008**, *49*, 2545–2556.
- (34) Srebalus, C.; Li, J.; Marshall, W. S.; Clemmer, D. E. *Anal. Chem.* **1999**, *71*, 3918–3927.
- (35) Trimpin, S.; Tan, B.; O'Dell, D. K.; Bohrer, B. C.; Merenbloom, S. I.; Pazos, M. X.; Clemmer, D. E.; Walker, J. M. *Int. J. Mass Spectrom.* **2009**, *287*, 58–69.
- (36) Sheehan, E. W.; Willoughby, R. C. Ion enrichment aperture arrays. U.S. Patent 7,060,976, 2006.